



Article

# Altered PPAR $\gamma$ Expression Promotes Myelin-Induced Foam Cell Formation in Macrophages in Multiple Sclerosis

Elien Wouters<sup>1</sup>, Elien Grajchen<sup>1</sup>, Winde Jorissen<sup>1</sup>, Tess Dierckx<sup>1</sup>, Suzan Wetzels<sup>2</sup>,  
Melanie Loix<sup>1</sup>, Marie Paule Tulleners<sup>1</sup>, Bart Staels<sup>3</sup> , Piet Stinissen<sup>1</sup>, Mansour Haidar<sup>1</sup>,  
Jeroen F.J. Bogie<sup>1</sup> and Jerome J.A. Hendriks<sup>1,\*</sup>

<sup>1</sup> Department of Immunology and Infection, Biomedical Research Institute, Hasselt University, 3590 Diepenbeek, Belgium; elien.wouters@uhasselt.be (E.W.); elien.grajchen@uhasselt.be (E.G.); winde.jorissen@gmail.com (W.J.); tess.dierckx@uhasselt.be (T.D.); melanie.loix@uhasselt.be (M.L.); mariepaule.tulleners@uhasselt.be (M.P.T.); piet.stinissen@uhasselt.be (P.S.); mansour.haidar@uhasselt.be (M.H.); Jeroen.Bogie@uhasselt.be (J.F.J.B.)

<sup>2</sup> Department of Pathology, CARIM, Maastricht University Medical Center, 6229 HX Maastricht, The Netherlands; suzan.wetzels@gmail.com

<sup>3</sup> University of Lille, Inserm, CHU Lille, Institut Pasteur de Lille, U1011-EGID, F-59000 Lille, France; bart.Staels@pasteur-lille.fr

\* Correspondence: jerome.hendriks@uhasselt.be

Received: 26 November 2020; Accepted: 3 December 2020; Published: 7 December 2020



**Abstract:** Macrophages play a crucial role during the pathogenesis of multiple sclerosis (MS), a neuroinflammatory autoimmune disorder of the central nervous system. Important regulators of the metabolic and inflammatory phenotype of macrophages are liver X receptors (LXRs) and peroxisome proliferator-activated receptors (PPARs). Previously, it has been reported that PPAR $\gamma$  expression is decreased in peripheral blood mononuclear cells of MS patients. The goal of the present study was to determine to what extent PPAR $\gamma$ , as well as the closely related nuclear receptors PPAR $\alpha$  and  $\beta$  and LXR $\alpha$  and  $\beta$ , are differentially expressed in monocytes from MS patients and how this change in expression affects the function of monocyte-derived macrophages. We demonstrate that monocytes of relapsing-remitting MS patients display a marked decrease in PPAR $\gamma$  expression, while the expression of PPAR $\alpha$  and LXR $\alpha/\beta$  is not altered. Interestingly, exposure of monocyte-derived macrophages from healthy donors to MS-associated proinflammatory cytokines mimicked this reduction in PPAR $\gamma$  expression. While a reduced PPAR $\gamma$  expression did not affect the inflammatory and phagocytic properties of myelin-loaded macrophages, it did impact myelin processing by increasing the intracellular cholesterol load of myelin-phagocytosing macrophages. Collectively, our findings indicate that an inflammation-induced reduction in PPAR $\gamma$  expression promotes myelin-induced foam cell formation in macrophages in MS.

**Keywords:** multiple sclerosis; myelin-loaded macrophages; inflammation; PPAR $\gamma$

## 1. Introduction

Multiple sclerosis (MS) is a neurodegenerative autoimmune disease of the central nervous system (CNS) characterized by chronic inflammation, demyelination, and axonal degeneration. During MS, circulating monocytes are recruited to the site of CNS inflammation. At the lesion site, monocyte-derived macrophages (MDMs) mediate demyelination and neurodegeneration [1]. Conversely, MDMs can also stimulate repair by internalizing myelin debris or by producing anti-inflammatory and repair-promoting factors [2–5]. After the internalization of myelin, cholesterol—the main lipid constituent of

myelin—is transported out of the cell via ATP-binding cassette transporters (e.g., ABCA1 and ABCG1) [6]. The efflux of cholesterol is essential to maintain intracellular lipid homeostasis and to prevent MDMs from becoming foamy. Nevertheless, a vast number of foamy macrophages containing abundant myelin remnants are found within demyelinating plaques of MS patients, indicating that lipid homeostasis is dysregulated in these cells [5,7].

Previously, we found that myelin uptake by bone marrow-derived mouse macrophages results in the activation of lipid sensing nuclear receptors (NRs), called peroxisome proliferator-activated receptors (PPARs) [8]. PPARs are ligand-activated transcription factors that control both lipid metabolism and inflammation [9]. Three PPAR isoforms have been identified, namely, PPAR $\alpha$  (NR1C1), PPAR $\beta/\delta$  (NR1C2), and PPAR $\gamma$  (NR1C3). Upon ligand binding, PPARs form heterodimers with retinoic X receptors (RXRs) and bind to specific DNA regions, called hormone response elements, resulting in the transcriptional regulation of target genes. PPAR activation in macrophages results in the active transcription of genes involved in lipid uptake, transport, synthesis, and efflux, thereby controlling cellular lipid homeostasis [10]. Additionally, PPAR activation inhibits proinflammatory signaling pathways [11].

It is previously reported that PPAR $\gamma$  protein level is decreased in peripheral blood mononuclear cells (PBMCs) of MS patients [12]. Furthermore, stimulation of PBMCs with phytohemagglutinin (PHA), a mitogen that stimulates inflammation, significantly reduces PPAR $\gamma$  protein abundance [12]. In this study, we demonstrate that the expression of PPAR $\gamma$  is decreased in monocytes of relapsing-remitting MS (RR-MS) patients and that MS-associated proinflammatory cytokines IFN $\gamma$  and IL1 $\beta$  reduce PPAR $\gamma$  expression. In addition, we find that PPAR $\gamma$  deficiency in myelin-containing macrophages has a significant impact on myelin processing by increasing the intracellular cholesterol load in these cells. Our findings highlight the importance of PPAR $\gamma$  in maintaining the intracellular lipid homeostasis in macrophages.

## 2. Results

### 2.1. The Inflammatory Environment in MS Reduces Macrophage PPAR $\gamma$ Expression

We determined to what extent PPAR $\gamma$ , as well as the closely related nuclear receptors PPAR $\alpha$ ,  $\beta$  and LXR $\alpha$ ,  $\beta$ , are differentially expressed in monocytes from MS patients. For this purpose, CD14 positive cells from age- and gender-matched healthy donors and MS patients were isolated. Our data show that the mRNA expression of PPAR $\gamma$ , but not LXR $\alpha$ , LXR $\beta$ , nor PPAR $\alpha$  was lower in monocytes of RR-MS patients compared to healthy donors (Figure 1A). No correlation of PPAR $\gamma$  expression with gender, disease activity, or therapy was observed in our samples. A negative correlation for LXR $\beta$  and age was found (Supplementary Figure S1). However, given the relatively small sample size, future studies should confirm the latter finding using a larger study cohort and identify possible correlations with other factors. No detectable levels of PPAR $\beta$  were found in control and MS patient-derived monocytes (undetermined Ct values). Interestingly, monocytes from secondary progressive (SP)-MS patients did not display a reduced expression of PPAR $\gamma$  (Supplementary Figure S2A). Furthermore, the reduced PPAR $\gamma$  expression in monocytes of RR-MS patients was lost upon differentiation into macrophages in vitro (Supplementary Figure S2B). These findings suggest that disease-associated factors present in RR-MS patients, but not in SP-MS patients and in vitro cultures, maintain reduced PPAR $\gamma$  expression in myeloid cells.

Given overt systemic inflammation in RR-MS patients compared to SP-MS patients, we next defined whether inflammation impacts the expression of the different LXR- and PPAR-isoforms. Our data show that the expression of PPAR $\gamma$  as well as PPAR $\alpha$  is suppressed by the inflammatory cytokines IFN $\gamma$  and IL1 $\beta$  in in vitro differentiated MDMs. In contrast, the expression of LXRs was not influenced by inflammatory cytokines (Figure 1B). To investigate the individual effect of both cytokines, cells were treated with either IFN $\gamma$  or IL1 $\beta$ . Here, we observed that IFN $\gamma$  most potently decreased PPAR $\gamma$  expression (Figure 1C). Taken together, these results strongly suggest that inflammation reduces

the expression of *PPARα* and *PPARγ* in myeloid cells of MS patients, and that *PPARγ* is most susceptible to the inhibitory impact of inflammatory mediators.

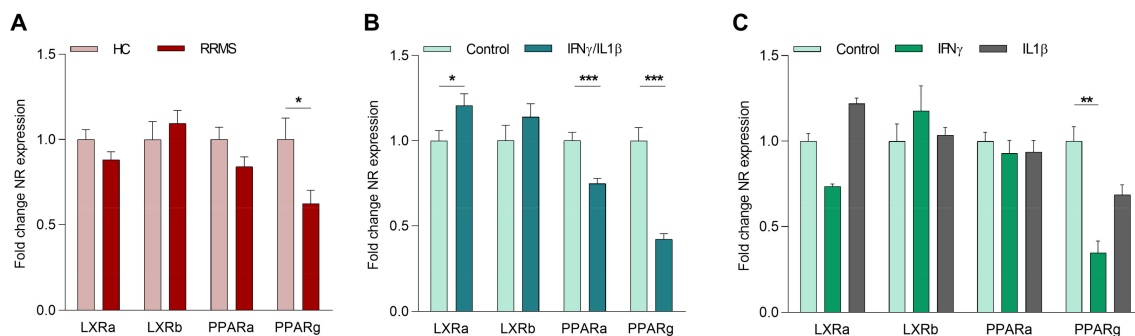


**Figure 1.** Inflammatory cytokines decrease *PPARγ* expression in macrophages. (A) Basal mRNA expression of *LXR*- and *PPAR*-isoforms in monocytes from age- and gender-matched healthy controls and relapsing-remitting multiple sclerosis (MS) patients ( $n = 15$ ). (B) Gene expression of *LXR*- and *PPAR*-isoforms in monocyte-derived macrophages (MDMs) from healthy controls stimulated with IFN $\gamma$ /IL1 $\beta$  ( $n = 11$ ). (C) Gene expression of *LXR*- and *PPAR*-isoforms in MDMs from healthy controls stimulated with IFN $\gamma$  or IL1 $\beta$  compared to nonstimulated cells ( $n = 4$ ). RR-MS = relapsing-remitting MS patient; NR = nuclear receptor. Values represent the mean  $\pm$  S.E.M. Statistical significance (A,B; unpaired Student's *t*-test, and C; one-way ANOVA with Dunn's multiple comparison correction) is indicated with asterisks: \*  $p \leq 0.05$ , \*\*  $p \leq 0.01$ , and \*\*\*  $p \leq 0.001$ .  $n$  represents the total number of donors included in the experiment.

## 2.2. Myelin Uptake Activates *PPARγ* in Phagocytes

In the CNS of MS patients, infiltrated monocytes differentiate into macrophages and actively phagocytose myelin [5]. Given that fatty acids are present in myelin and are well-known endogenous ligands of PPARs, we next sought to determine if altered *PPARγ* activity affects the physiology of myelin-phagocytosing macrophages. For this purpose, we first determined whether myelin internalization activates *PPARγ* in these cells. To this end, MDMs from healthy donors (HCs) were exposed to isolated human myelin and/or the *PPARγ* specific agonist (rosiglitazone) and antagonist (GW9662). First, *PPARγ* activation through its ligand-binding domain was studied using a GAL-4-*PPARγ* LBD chimera reporter assay in cells treated with myelin for 24 h. As depicted in Figure 2A, myelin treatment resulted in a 2-fold increase in *PPARγ* activity. Given that in vitro differentiation into macrophages abolishes the reduced *PPARγ* expression observed in monocytes of RR-MS patients (Supplementary Figure S2B), and the fact that monocytes are notoriously inefficient phagocytes, we were unable to study the direct impact of reduced PPAR signaling in MS-derived monocytes on their function. Therefore, we studied if the PPAR antagonist GW9662 altered the macrophage response to myelin. Myelin induced the expression of the PPAR responsive genes *perilipin 2* (*PLIN2*) and *stearoyl-CoA desaturase-1* (*SCD1*). This induction was reduced by GW9662 (Figure 2B). While *ABCG1* expression was also increased upon myelin internalization, this did not depend on *PPARγ* activation (Figure 2B). Of interest, myelin also increased the expression of *PPARγ* (Figure 2C), suggesting a positive feedback loop that augments *PPARγ* signaling. The expression of *PLIN2*, *SCD1*, and *ABCG1* was also increased upon rosiglitazone treatment, confirming that these genes are regulated through *PPARγ* (Figure 2D). Next, we defined if an inflammatory environment and the consequent reduction in *PPARγ* expression impacts the capacity of myelin to induce *PPARγ* and the *PPARγ*-responsive gene *PLIN2* in MDMs from HCs. Our data demonstrate that myelin does not significantly induce *PPARγ* and *PLIN2* expression under inflammatory conditions (Figure 2E). Collectively, these data illustrate that myelin internalization results in the activation of *PPARγ*, and that the inflammation-associated reduction in *PPARγ* expression reduces the capacity of myelin to (auto)regulate *PPARγ* and *PLIN2* expression.

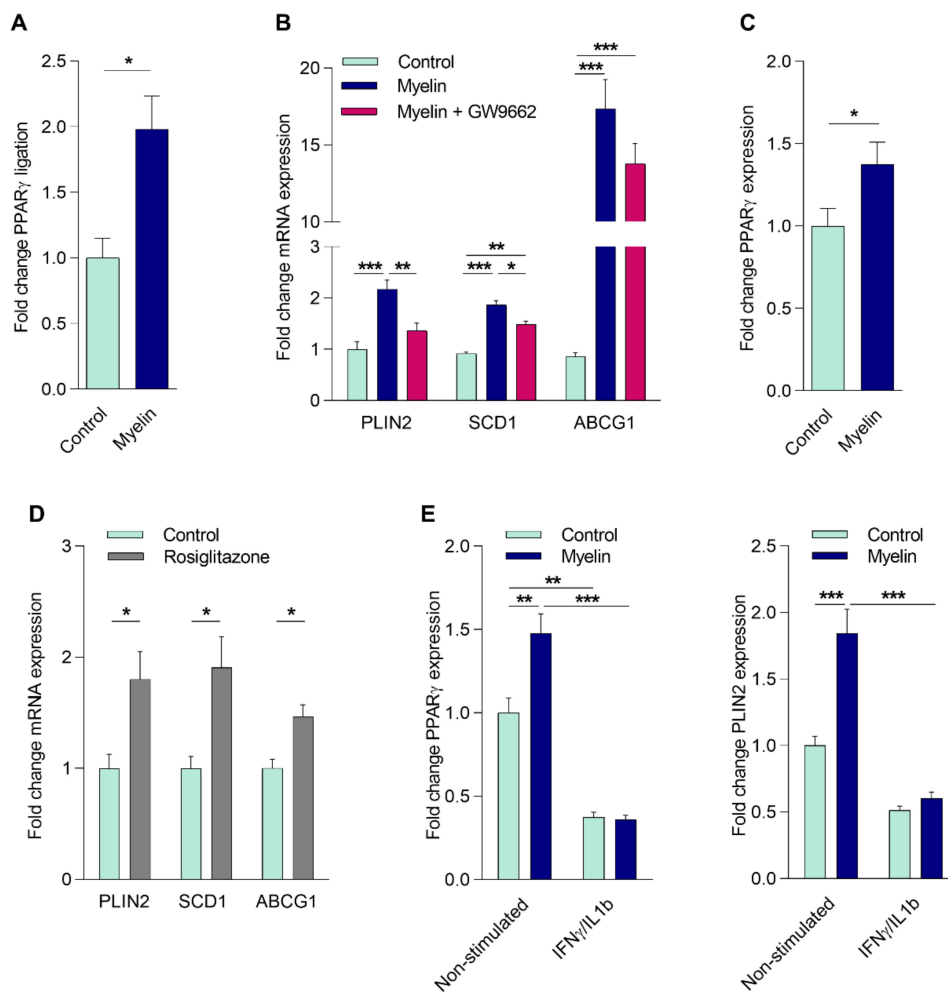


**Figure 2.** Myelin uptake activates PPAR $\gamma$  in phagocytes. (A) CHME3 cells treated with myelin or left untreated. PPAR $\gamma$  ligand-binding activity was determined using the GAL-4-PPAR $\gamma$  chimera assay system ( $n = 5$ ). (B) mRNA expression of PPAR $\gamma$  response genes in MDMs from healthy controls (HCs) stimulated with myelin in the presence or absence of GW9662 (25  $\mu$ M;  $n = 8$ ). (C) PPAR $\gamma$  mRNA expression in MDMs from HCs treated with myelin compared to non-stimulated cells ( $n = 11$ ). (D) mRNA expression of PPAR $\gamma$  response genes in MDMs from HCs stimulated with rosiglitazone (1  $\mu$ M;  $n = 9$ ). (E) PPAR $\gamma$  and perilipin 2 (PLIN2) expression in MDMs from HCs treated with IFN $\gamma$ /IL1 $\beta$ , followed with or without stimulation with myelin ( $n = 6$ ). Values represent the mean  $\pm$  S.E.M. Statistical significance (A,C,D; Mann–Whitney test, B; one-way ANOVA with Tukey’s multiple comparison correction, and E; two-way ANOVA with Sidak’s multiple comparison correction) is indicated with asterisks: \*  $p \leq 0.05$ , \*\*  $p \leq 0.01$ , and \*\*\*  $p \leq 0.001$ .  $n$  represents the total number of biological replicates (A) or donors (B–E) included in the experiment.

### 2.3. Myelin Controls the Inflammatory Phenotype of Macrophages Independently of PPAR $\gamma$

Ample evidence indicates that myelin internalization modulates inflammatory gene expression in macrophages [8,13]. As PPAR $\gamma$  is well-known to suppress the inflammatory status of macrophages [11], we next defined whether PPAR $\gamma$  activation impacts the inflammatory phenotype of myelin-containing macrophages (mye-macrophages) [11]. Our data show that myelin uptake decreased TNF $\alpha$  expression, both on mRNA and protein level, in MDMs from healthy donors. However, this decrease did not reach statistical significance. In contrast, the PPAR $\gamma$  agonist rosiglitazone reduced IL6 expression (mRNA and protein), without affecting TNF $\alpha$  expression (Figure 3A,B). These results suggest that PPAR $\gamma$  is not the main regulator of myelin-induced changes in inflammatory gene expression. To confirm that myelin impacts the inflammatory phenotype in a PPAR $\gamma$ -independent manner, myelin-treated MDMs

from HCs were exposed to the PPAR $\gamma$  antagonist GW9662. Inhibiting PPAR $\gamma$  activity did not change the expression of *TNF $\alpha$*  and *IL6* in myelin-treated MDMs, providing further evidence for the redundant role of PPAR $\gamma$  in driving the expression of these inflammatory genes in myel-macrophages (Figure 3C). Taken together, these data demonstrate that myelin uptake does not change the inflammatory phenotype of macrophages through the activation of PPAR $\gamma$ .

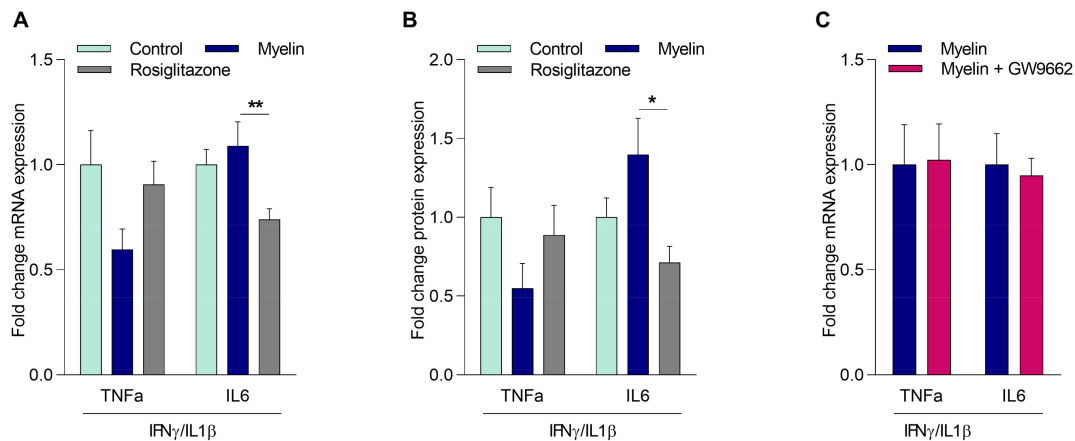


**Figure 3.** Myelin controls the inflammatory phenotype of myel-macrophages independently of PPAR $\gamma$ . MDMs from HCs treated with myelin, rosiglitazone, or left untreated, followed by incubation with IFN $\gamma$ /IL1 $\beta$  ( $n = 6$ ). *TNF $\alpha$*  and *IL6* mRNA expression levels (A) and protein expression levels (B) were detected. (C) *TNF $\alpha$*  expression in MDMs from HCs treated with myelin in the presence or absence of GW9662, followed by incubation with IFN $\gamma$ /IL1 $\beta$  ( $n = 4$ ). Values represent the mean  $\pm$  S.E.M. Statistical significance (A,B; one-way ANOVA with Dunn's multiple comparison correction, and C; Mann–Whitney test) is indicated with asterisks: \*  $p \leq 0.05$ , and \*\*  $p \leq 0.01$ .  $n$  represents the total number of donors included in the experiment.

#### 2.4. Reduced PPAR $\gamma$ Activity Does Not Impact Myelin Phagocytosis but Hampers Intracellular Lipid Processing

MDMs of MS patients have a reduced capacity to phagocytose myelin [14]. As PPARs control the expression of phagocytic receptors involved in the uptake of myelin such as cluster of differentiation 36 (CD36) and scavenger receptor-A1 (SR-A1) [15,16], we assessed whether PPAR $\gamma$  controls myelin phagocytosis. First, we examined whether myelin-induced PPAR $\gamma$  activation increases the expression of *CD36* or *SR-A1*. By treating MDMs from healthy donors with myelin in the absence or presence of the PPAR $\gamma$  antagonist, we show that PPAR $\gamma$  did not significantly influence *CD36* or *SR-A1* mRNA expression in MDMs upon myelin uptake (Figure 4A). Next, the effect of PPAR $\gamma$  deficiency on the phagocytosis of myelin was determined. For this purpose, MDMs from HCs were exposed to DiI-labeled myelin in the presence or absence of GW9662. No change in DiI myelin phagocytosis was observed when PPAR $\gamma$  was inhibited (Figure 4B). These findings indicate that PPAR $\gamma$  does not regulate myelin internalization. A vast number of foamy macrophages containing abundant myelin remnants are found within demyelinating plaques of MS patients. Since PPAR $\gamma$  has been reported to be a crucial mediator of lipid processing [17,18], we next determined the effect of a reduced PPAR $\gamma$  activity on lipid storage after myelin uptake. By means of the Amplex<sup>TM</sup> Red Cholesterol Assay, more cholesteryl esters (CEs) were detected inside myel-macrophages from HCs when PPAR $\gamma$  was inhibited (Figure 4C). In line with these results, an increased amount of lipid droplets (LDs) was observed in cells treated with the PPAR $\gamma$  antagonist after myelin uptake (Figure 4D). Similar as before, inefficient phagocytosis by monocytes and the negating effect of monocyte differentiation into macrophages on PPAR $\gamma$  expression did not allow us to confirm these findings directly in MS patient-derived monocytes and macrophages. Collectively, these data indicate that a reduced PPAR $\gamma$  activity promotes the formation of foamy macrophages without affecting the uptake of myelin.

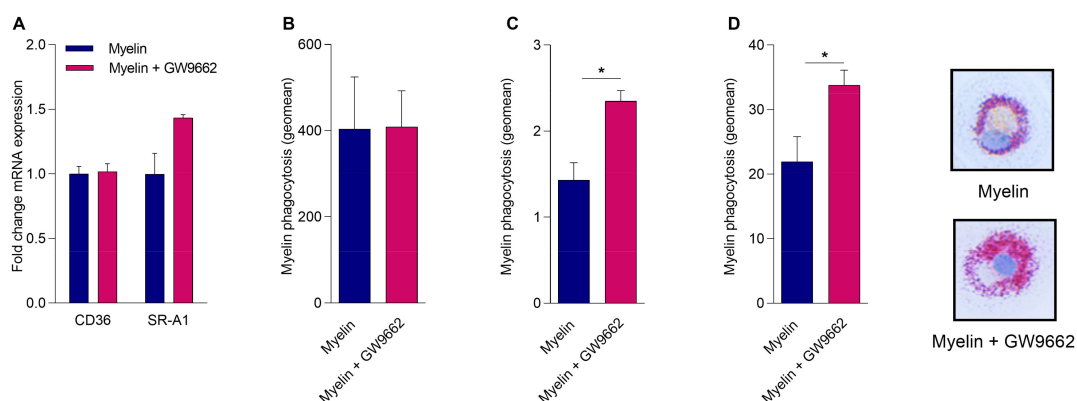


**Figure 4.** PPAR $\gamma$  controls the formation of lipid droplets in myel-macrophages but does not impact myelin phagocytosis. (A) cluster of differentiation 36 (*CD36*) and scavenger receptor-A1 (*SR-A1*) expression in MDMs from HCs pretreated with GW9662 or DMSO, followed by an incubation with myelin ( $n = 5$ ). (B) DiI myelin phagocytosis by MDMs from HCs preincubated with GW9662 or DMSO ( $n = 4$ ). (C) MDMs from HCs incubated with myelin in the absence or presence of GW9662. Cholesteryl esters (CE) load was measured using the Amplex<sup>TM</sup> Red Cholesterol Assay ( $n = 4$ ). (D) MDMs from HCs incubated with myelin in the absence or presence of GW9662. Neutral lipids were stained and quantified using Oil red O (ORO) ( $n = 5$ ). Values represent the mean  $\pm$  S.E.M. Statistical significance (Mann–Whitney test) is indicated with asterisks: \*  $p \leq 0.05$ .  $n$  represents the total number of donors included in the experiment.

### 3. Discussion

The activation of NRs such as LXRs and PPARs suppresses neuroinflammation by changing the metabolic and inflammatory properties of immune cells. Here, we show that an inflammation-induced reduction in PPAR $\gamma$  expression promotes myelin-induced foam cell formation in macrophages, which may negatively impact MS lesion progression.

Diverse studies demonstrated that inflammatory cytokine levels in biological fluids correlate with disease activity and the occurrence of relapses in MS patients [19,20]. Interestingly, our findings show that MS-associated inflammatory mediators reduce the expression of PPAR $\gamma$ , mimicking the PPAR $\gamma$  expression profile of monocytes in RR-MS patients. More specifically, IFN $\gamma$  most prominently reduced PPAR $\gamma$  expression. IFN $\gamma$  is secreted by activated immune cells, including Th1-cells, and is highly elevated in the serum and cerebrospinal fluid (CSF) of MS patients, as well as inside MS lesions [21,22]. Genetic ablation of IFN $\gamma$  aggravates the disease course in experimental autoimmune encephalomyelitis (EAE), a well-established animal model of MS [23]. However, when IFN $\gamma$  administration was tested as a clinical drug in MS patients, it resulted in an exacerbation of the disease activity [24,25]. Considering the protective impact of PPAR $\gamma$  activation on neuroinflammation, it is tempting to speculate that IFN $\gamma$  partially promotes disease severity by reducing monocytic PPAR $\gamma$  expression. Our findings are in line with a previous study that showed that PPAR $\gamma$  expression is decreased in PBMCs of MS patients [12]. Collectively, our data show that the proinflammatory environment that is typically associated with MS decreases PPAR $\gamma$ , thereby potentially promoting MS disease progression.

PPAR $\gamma$  agonists are well-known to ameliorate disease activity in mice with EAE. In these animals, PPAR $\gamma$  activation reduces CNS inflammation by decreasing the expression of proinflammatory cytokines, including TNF $\alpha$  and IL6 [26–28]. In macrophages, PPAR $\gamma$  activation results in the retention of the NCoR corepressor complex at the promoter region of NF-kB target genes, keeping the expression of inflammatory genes in a repressed state [11]. Here, we demonstrate that myelin internalization increases the transcriptional activity of PPAR $\gamma$  in human macrophages. Nonetheless, phenotypic analysis showed that myelin impacts the inflammatory features of myel-macrophages in a PPAR $\gamma$ -independent manner. Based on these findings, the activation of other NRs likely explains the observed effects of myelin on the inflammatory phenotype of macrophages in our study. With respect to the latter, in a previous

study we reported that myelin suppresses the inflammatory properties of myelin-containing mouse macrophages in a PPAR $\beta/\delta$ - and LXR-dependent manner [6,8,29]. Collectively, these findings indicate that myelin activates PPAR $\gamma$  but that this activation does not impact the inflammatory phenotype of human macrophages.

Inefficient clearance of myelin debris inhibits oligodendrocyte precursor cell differentiation. Hence, adequate uptake of myelin debris is essential for remyelination to occur [3,30]. Macrophages phagocytose myelin via scavenger receptors including CD36 and SR-A1 [16,31]. Although CD36 and SR-A1 expression is transcriptionally regulated by PPAR $\gamma$  [15,16], we show that myelin uptake does not increase *CD36* or *SR-A1* expression in macrophages, nor did PPAR $\gamma$  inhibition reduce the phagocytosis of myelin. In contrast to our findings, a study by Natrajan et al. demonstrated that PPAR $\gamma$  activation increases the uptake of myelin [32]. However, in the latter study the authors made use of synthetic PPAR $\gamma$  agonists to show that PPAR $\gamma$  activation has an additive effect on myelin phagocytosis. Here, we utilized a PPAR $\gamma$  antagonist to define the role of endogenous PPAR $\gamma$  activity in myelin uptake. Thus, our findings indicate that the reduced myeloid cell expression of PPAR $\gamma$  in RR-MS patients probably does not impact the capacity of these cells to internalize myelin debris.

Alongside controlling the phagocytic and inflammatory features of macrophages, PPAR $\gamma$  mediates the intracellular processing and efflux of lipids. In macrophages present in atherosclerotic plaques, PPAR $\gamma$  activation results in an increase in cholesterol efflux, and ultimately a reduction in foam cell formation [33]. The presence of foamy macrophages is also a characteristic of active MS lesions, indicating dysregulation of lipid metabolism inside these cells. Interestingly, we recently found that sustained intracellular accumulation of myelin debris in macrophages induces a highly inflammatory transcriptional profile [13]. Here, we demonstrate that myelomacrophages display a marked increase in LDs when PPAR $\gamma$  activity is reduced. This increase in LDs could be the result of a decrease in lipid processing or efflux [18]. At the level of lipid processing, PPAR-stimulation induces mitochondrial  $\beta$ -oxidation of fatty acids (FAs) via increasing the expression of carnitine palmitoyl transferase (CPT)1 [34]. A reduction in mitochondrial  $\beta$ -oxidation increases the availability of FAs for neutral lipid synthesis, thereby augmenting lipid droplet formation [35]. Additionally, PPAR activation induces reverse cholesterol transport by increasing the expression of ABCA1, ABCG1, and SR-B1 [18,36,37]. Blocking this efflux will result in the buildup of free cholesterol inside the cell which will be esterified and stored inside LDs to protect the cell from lipotoxicity. However, we did not find a difference in *ABCA1* and *ABCG1* mRNA expression after blocking PPAR $\gamma$  activity. Nevertheless, further research is necessary to study the expression and localization of these transporters at the protein level.

While our findings link decreased PPAR $\gamma$  expression to inflammation, levels of PPAR $\gamma$  and PLIN2 have been reported to be elevated in the spinal cord of EAE mice and in the CSF of MS patients [38,39]. This induction in PPAR $\gamma$  expression might reflect an endogenous protective mechanism to counteract the proinflammatory response during MS or an increase in infiltrating macrophages that express high levels of PPAR $\gamma$ . We show that the expression of LD-associated protein *PLIN2* is increased after PPAR $\gamma$  stimulation. *PLIN2* is important for the stability of LDs in macrophages. Nevertheless, myelomacrophages display a marked increase in LDs when PPAR $\gamma$  activity is blocked. These findings indicate that either other factors in the lesion environment impact *PLIN2* expression, or that PPARs also control other (unidentified) processes that contribute to LD processing and biogenesis (e.g.,  $\beta$ -oxidation and cholesterol efflux). Therefore, more research is warranted to unravel the molecular mechanisms that underlie the impact of PPAR $\gamma$  on the accumulation of LDs in myelomacrophages.

We found that differentiation of monocytes into macrophages *in vitro* nullifies the reduced PPAR $\gamma$  expression observed in monocytes of RR-MS patients. This finding confirms that the inflammatory microenvironment in RR-MS is essential for maintaining reduced PPAR $\gamma$  activation. This indicates that when inflammatory mediator production is resolved in MS lesions, PPAR function in macrophages will be restored. In future studies, it would be of interest to confirm these findings in post-mortem inflammatory and noninflammatory lesions of MS patients, or compare foamy phagocyte physiology

in MS patients to individuals affected by non- or less-inflammatory demyelinating disorders such as adrenoleukodystrophy.

In conclusion, we report that PPAR $\gamma$  deficiency in myeloid macrophages results in an increased intracellular lipid load. This study brings us closer to understanding the mechanisms by which PPAR $\gamma$  can modulate macrophage function and MS lesion progression, and may help in the development of therapeutic strategies to target MS.

## 4. Materials and Methods

### 4.1. Human Subjects

This study was approved by the Medical Ethics Committees of Hasselt University and UZ Leuven (UH-VAISMS-P1/S56441; March 2014). Written informed consent was obtained from all donors. A total of 22 HCs, 15 RR-MS patients, and 7 SP-MS patients were included in the study (Supplementary Table S1). RR-MS patients participating in the study were in remission at the time of sampling. MS patients were included independent of their treatment. Exclusion criteria for HCs and patients were reported hypercholesterolemia, cardiovascular diseases, diabetes, pregnancy, cancer, liver disease, and treatment with cholesterol modifying agents.

### 4.2. Cell Culture

PBMCs were isolated from whole blood using density gradient centrifugation, as previously described [40]. CD14<sup>+</sup> monocytes were collected by positive selection according to the manufacturer's guidelines (Stemcell Technologies, Grenoble, France). MDMs were obtained by culturing isolated monocytes ( $2 \times 10^6$  cells/mL) in MDM culture medium (DMEM-high glucose medium (Sigma-Aldrich, Diegem, Belgium) supplemented with 10% human serum (Sigma-Aldrich), 50 U/mL penicillin, 50 U/mL streptomycin, and 2 mM L-glutamine (Sigma-Aldrich)) at 37 °C, 5% CO<sub>2</sub>. After 7 days, MDMs were collected using PBS/EDTA (10 mM) and plated at  $0.5 \times 10^6$  cells/mL in MDM culture medium.

### 4.3. Human Myelin Isolation

Myelin was isolated from post-mortem nondemented human brain using sucrose density-gradient centrifugation, as previously described [41]. Briefly, tissue was homogenized in 0.32 M sucrose and layered over 0.85 M sucrose. The homogenate was ultra-centrifuged ( $75,000 \times g$ , 4 °C, 30 min) and crude myelin was collected from the interface. The collected myelin was washed in ddH<sub>2</sub>O and subjected to osmotic disintegration. A second sucrose density-gradient centrifugation was carried out by dissolving the pellet in 0.32 M sucrose and layering it on top of 0.85 M sucrose. After ultracentrifugation ( $75,000 \times g$ , 4 °C, 30 min), the myelin-containing interface was collected, washed in ddH<sub>2</sub>O, and dissolved in PBS. Myelin protein concentration was measured using the BCA protein assay kit (Thermo Fisher Scientific, Erembodegem, Belgium). The amount of endotoxin was determined using the Chromogenic Limulus Amebocyte Lysate assay kit (Genscript Incorporation, Aachen, Germany). Isolated myelin contained a negligible amount of endotoxin ( $\leq 1.8 \times 10^{-3}$  pg/ $\mu$ g myelin) [42].

### 4.4. Macrophage Stimulation and Pharmacological Treatments

The effect of a proinflammatory environment on mRNA expression was measured by treating cells with IFN $\gamma$  and/or IL1 $\beta$  (100 ng/mL, PeproTech, London, UK) for 6 h. To study PPAR $\gamma$  expression and activity, MDMs were stimulated with myelin (100  $\mu$ g/mL), rosiglitazone (PPAR $\gamma$  agonist, 1  $\mu$ M, Sigma-Aldrich), or dimethylsulfoxide (DMSO; Leuven, Belgium) for 24 h, in the presence or absence of the PPAR $\gamma$  antagonist, GW9662 (25  $\mu$ M, Sigma-Aldrich) or IFN $\gamma$ /IL1 $\beta$  (100 ng/mL). Inflammatory gene expression was measured after treating cells with myelin (100  $\mu$ g/mL) or rosiglitazone (1  $\mu$ M) for 18 h, followed by incubation with IFN $\gamma$ /IL1 $\beta$  (100 ng/mL) for 6 h. GW9662 (25  $\mu$ M) was added to the



myelin conditions to study the involvement of PPAR $\gamma$  in myelin-induced suppression of inflammatory gene expression.

#### 4.5. RNA Extraction and Real-Time Quantitative PCR (RT-qPCR)

Total RNA was isolated with Qiazol (Qiagen, Venlo, The Netherlands) and the RNeasy mini kit (Qiagen), according to the manufacturer's guidelines. A NanoDrop spectrophotometer (Isogen Life Science, De Meern, The Netherlands) was used to determine RNA concentration and purity. RNA was reverse-transcribed using qScript<sup>TM</sup> cDNA SuperMix (Quanta Biosciences, VWR, Leuven, Belgium) according to the manufacturer's instructions. RT-qPCR was conducted on a Step One Plus detection system (Applied biosystems, Foster City, CA, USA). Cycle conditions were 95 °C for 20 s, followed by 40 cycles of 95 °C for 3 s, and 60 °C for 30 s. The PCR reaction mixture contained SYBR green master mix (Thermo Fisher Scientific), 0.3  $\mu$ M forward and reverse primer (IDT technologies, Leuven, Belgium), RNase free water, and 12.5 ng cDNA template in a total reaction volume of 10  $\mu$ L. Relative quantitation of gene expression was accomplished using the comparative Ct method. Data were normalized to the most stable reference genes. Primers used for RT-qPCR are shown in Supplementary Table S2.

#### 4.6. Enzyme-Linked Immunosorbent Assay (ELISA)

MDMs were pretreated for 18 h with myelin (100  $\mu$ g/mL), rosiglitazone (1  $\mu$ M), or DMSO, followed by an incubation with IFN $\gamma$ /IL1 $\beta$  (100 ng/mL) for 24 h. Afterwards, medium was collected, centrifuged at 1400 rpm for 10 min, and diluted 1/10. TNF $\alpha$  and IL6 protein expression was measured using ELISA (eBioscience, San Diego, CA, USA). Absorbance was determined by a microplate reader (BIORAD iMark<sup>TM</sup> Microplate Reader, Temse, Belgium) at 450 nm.

#### 4.7. Luciferase Assay

Human CHME3 microglial cells were cultured in DMEM-high glucose medium supplemented with 10% fetal bovine serum (Invitrogen, Merelbeke, Belgium), 50 U/mL penicillin, and 50 U/mL streptomycin at 37 °C, 5% CO<sub>2</sub>. CHME3 cells were transfected overnight with plasmids using JetPEI<sup>®</sup> transfection reagent (Polyplus, Illkirch, France), according to the manufacturer's protocol. Plasmids used for transfection encoded for pG5-TK-GL3 (GAL5), pCMV-Bgal, and PPAR $\gamma$  (kindly provided by Prof. dr. Bart Staels, University of Lille, France). Following transfection, cells were serum starved for 5 h. Afterwards, CHME3 cells were treated with myelin (100  $\mu$ g/mL, 24 h) and lysed in lysis buffer (25 mM Gly-Gly (Sigma-Aldrich), 1% Triton (Sigma-Aldrich), 15 mM MgSO<sub>4</sub> (Sigma-Aldrich), and 4 mM EGTA (Sigma-Aldrich)). Ligation of myelin components to PPAR $\gamma$  was measured using the ONE-Glo<sup>TM</sup> Luciferase Assay System kit (Promega, Leiden, The Netherlands). Luminescence was determined with the FLUOstar optima microplate reader (BMG Labtech, Ortenberg, Germany). To study transfection efficacy,  $\beta$ -galactosidase was measured using B-gal buffer (80% Buffer Z (100 mM Na<sub>2</sub>HPO<sub>4</sub>, 10 mM KCl, 1 mM MgSO<sub>4</sub>, 0.05 mM 2-mercaptoethanol) and 20% ONGP buffer (13.28 mM ONGP, 82 mM Na<sub>2</sub>HPO<sub>4</sub>, 18 mM NaH<sub>2</sub>PO<sub>4</sub>). Absorbance was determined at 410 nm by the FLUOstar optima microplate reader.

#### 4.8. Flow Cytometry

To study myelin phagocytosis, isolated myelin (10 mg/mL) was fluorescently labelled with 12.5  $\mu$ g/mL 1,1''-diotadecyl-3,3,3',3',-tetramethylindocarbocyanide perchlorate (DiI; Sigma-Aldrich) for 30 min at 37 °C, as previously described [43]. MDMs were pretreated with GW9662 (25  $\mu$ M) or DMSO for 30 min, followed by an incubation with DiI-labeled myelin (100  $\mu$ g/mL, 1.5 h) at 37 °C, 5% CO<sub>2</sub>. DiI fluorescence was measured using a FACS Calibur flow cytometer (BD biosciences, Erembodegem, Belgium).

#### 4.9. Cholesteryl Ester (CE) Determination

MDMs were preincubated with GW9662 (25  $\mu$ M) or DMSO for 30 min, followed by an incubation with myelin (100  $\mu$ g/mL) for 24 h. CEs were measured using the Amplex<sup>TM</sup> Red Cholesterol Assay Kit (Thermo Fisher Scientific), according to manufacturer's instructions. Briefly, cells were washed twice with PBS after treatment and lysed in Amplex<sup>TM</sup> Red reaction buffer. Amplex<sup>TM</sup> Red working solution, with or without cholesterol esterase was added to the cell lysate and incubated at 37 °C protected from light. After 30 min, fluorescence was measured at an excitation wavelength of 540 nm and an emission wavelength of 590 nm using the FLUOstar optima microplate reader. CE concentration was calculated by subtracting free cholesterol concentration from total cholesterol concentration.

#### 4.10. Oil Red O (ORO) Staining and Quantification

MDMs were preincubated with GW9662 (25  $\mu$ M) or DMSO for 30 min, followed by an incubation with myelin (100  $\mu$ g/mL) for 24 h. Cells were fixed in 4% paraformaldehyde (Sigma-Aldrich) for 20 min at RT. Neutral lipids were stained using ORO (Sigma-Aldrich) in 60% isopropanol for 10 min. Following incubation, unbound particles were washed away with deionized water. For the ORO staining, coverslips were counterstained with Mayer's hematoxylin for 60 s to visualize nuclei. Afterwards, cells were rinsed in running tap water and mounted on microscope slides with aqueous mounting solution. Representative images were taken using a Leica DM2000 LED microscope (Leica Microsystems, Wetzlar, Germany). For ORO quantification, ORO was extracted by incubating the cells with isopropanol for 10 min, while shaking. Absorbance was measured using a microplate reader (BIORAD iMark<sup>TM</sup> Microplate Reader) at 510 nm.

#### 4.11. Statistical Analysis

MS patients were diagnosed based on the 2017 McDonald criteria [44]. Multiple linear regression models for each dependent response variable were fitted using SPSS Statistics 25.0 (SPSS, Chicago, IL, USA). A backward-elimination approach was performed in each multiple linear regression model until all remaining variables had  $p < 0.05$ . Data were statistically analyzed using GraphPad Prism v6 (GraphPad Software, La Jolla, CA, USA) and are reported as mean  $\pm$  standard error of the mean (S.E.M.). D'Agostino-Pearson omnibus normality test was used to test normal distribution. One-way analysis of variance (ANOVA) with Tukey's multiple comparison correction, two-way ANOVA with Sidak's multiple comparison correction, or two-tailed unpaired Student's *t*-test were used for normally distributed data sets. The Mann-Whitney analysis or one-way ANOVA with Dunn's multiple comparison correction was used for data sets which did not pass normality. \*  $p \leq 0.05$ , \*\*  $p \leq 0.01$ , and \*\*\*  $p \leq 0.001$ .

**Supplementary Materials:** The following supplementary materials are available online at <http://www.mdpi.com/1422-0067/21/23/9329/s1>, Figure S1: Negative correlation for LXR $\beta$  and age, Figure S2: Nuclear receptor expression in monocytes of SP-MS patients and in vitro differentiated monocyte-derived macrophages, Table S1: Descriptive statistics for the study population, Table S2: List of primer sequences used for RT-qPCR.

**Author Contributions:** Conceptualization, E.W., J.F.J.B. and J.J.A.H.; formal analysis, E.W.; funding acquisition, P.S., J.F.J.B. and J.J.A.H.; investigation, E.W., E.G., W.J., T.D., S.W., M.L. and M.P.T.; methodology, E.W., J.F.J.B. and J.J.A.H.; project administration, E.W.; resources, B.S. and J.J.A.H.; supervision, J.F.J.B. and J.J.A.H.; validation, E.W.; writing—original draft, E.W.; writing—review and editing, M.H., J.F.J.B. and J.J.A.H. All authors have read and agreed to the published version of the manuscript.

**Funding:** This research received no external funding.

**Conflicts of Interest:** The authors declare no conflict of interest.

#### Abbreviations

ABCA1	ATP-binding cassette transporter A1
ABCG1	ATP-binding cassette transporter G1
ANOVA	Analysis of variance

CD36	Cluster of differentiation 36
CE	Cholesteryl ester
CNS	Central nervous system
CPT1	Carnitine palmitoyl transferase 1
CSF	Cerebrospinal fluid
DiI	1,1''-diotadecyl-3,3,3',3',-tetramethylindocarbocyanide perchlorate
DMSO	Dimethylsulfoxide
EAE	Experimental autoimmune encephalomyelitis
ELISA	Enzyme-linked immunosorbent assay
FA	Fatty acids
HC	Healthy control
LD	Lipid droplet
LXR	Liver X receptor
MDM	Monocyte-derived macrophage
MS	Multiple sclerosis
NCoR	Nuclear receptor co-repressor
NR	Nuclear receptor
ORO	Oil red O
PBMC	Peripheral blood mononuclear cell
PHA	Phytohemagglutinin
PLIN2	Perilipin 2
PPAR	Peroxisome proliferator-activated receptor
RR-MS	Relapsing-remitting MS
RT-qPCR	Real-time quantitative PCR
RXR	Retinoid X receptor
SCD1	Stearoyl-CoA desaturase-1
S.E.M.	Standard error of the mean
SP-MS	Secondary progressive MS
SR-A1	Scavenger receptor-A1
SR-B1	Scavenger receptor-B1

## References

1. Bogie, J.F.; Stinissen, P.; Hendriks, J.J. Macrophage subsets and microglia in multiple sclerosis. *Acta Neuropathol.* **2014**, *128*, 191–213. [[CrossRef](#)]
2. Jiang, Z.; Jiang, J.X.; Zhang, G.X. Macrophages: A double-edged sword in experimental autoimmune encephalomyelitis. *Immunol. Lett.* **2014**, *160*, 17–22. [[CrossRef](#)] [[PubMed](#)]
3. Kotter, M.R.; Zhao, C.; van Rooijen, N.; Franklin, J.M.R. Macrophage-depletion induced impairment of experimental CNS remyelination is associated with a reduced oligodendrocyte progenitor cell response and altered growth factor expression. *Neurobiol. Dis.* **2005**, *18*, 166–175. [[CrossRef](#)] [[PubMed](#)]
4. Nally, F.K.; De Santi, C.; McCoy, C.E. Nanomodulation of macrophages in multiple sclerosis. *Cells* **2019**, *8*, 543. [[CrossRef](#)] [[PubMed](#)]
5. Grajchen, E.; Hendriks, J.J.A.; Bogie, J.F.J. The physiology of foamy phagocytes in multiple sclerosis. *Acta Neuropathol. Commun.* **2018**, *6*, 124. [[CrossRef](#)]
6. Bogie, J.F.; Timmermans, S.; Huynh-Thu, V.A.; Irrthum, A.; Smeets, J.M.H.; Gustafsson, J.-A.; Steffensen, K.R.; Mulder, M.; Stinissen, P.; Hellings, N. Myelin-derived lipids modulate macrophage activity by liver X receptor activation. *PLoS ONE* **2012**, *7*, e44998. [[CrossRef](#)]
7. Kuhlmann, T.; Ludwin, S.; Prat, A.; Antel, J.; Bruck, W.; Lassmann, H. An updated histological classification system for multiple sclerosis lesions. *Acta Neuropathol.* **2017**, *133*, 13–24. [[CrossRef](#)]
8. Bogie, J.F.; Jorissen, W.; Mailleux, J.; Nijland, P.G.; Zelcer, N.; Vanmierlo, T.; Van Horssen, J.; Stinissen, P.; Hellings, N.; Hendriks, J.J.A. Myelin alters the inflammatory phenotype of macrophages by activating PPARs. *Acta Neuropathol. Commun.* **2013**, *1*, 43. [[CrossRef](#)]
9. Bensinger, S.J.; Tontonoz, P. Integration of metabolism and inflammation by lipid-activated nuclear receptors. *Nature* **2008**, *454*, 470–477. [[CrossRef](#)]

10. Rigamonti, E.; Chinetti-Gbaguidi, G.; Staels, B. Regulation of macrophage functions by PPAR-alpha, PPAR-gamma, and LXRs in mice and men. *Arterioscler. Thromb. Vasc. Biol.* **2008**, *28*, 1050–1059. [[CrossRef](#)]
11. Bougarne, N.; Weyers, B.; Desemet, S.J.; Deckers, J.; Ray, D.W.; Staels, B.; De Bosscher, K. Molecular actions of PPARalpha in lipid metabolism and inflammation. *Endocr. Rev.* **2018**, *39*, 760–802. [[CrossRef](#)] [[PubMed](#)]
12. Klotz, L.; Schmidt, M.; Giese, T.; Sastre, M.; Knolle, P.; Klockgether, T.; Heneka, M.T. Proinflammatory stimulation and pioglitazone treatment regulate peroxisome proliferator-activated receptor gamma levels in peripheral blood mononuclear cells from healthy controls and multiple sclerosis patients. *J. Immunol.* **2005**, *175*, 4948–4955. [[CrossRef](#)] [[PubMed](#)]
13. Bogie, J.F.J.; Grajchen, E.; Wouters, E.; Corales Garcia, A.; Dierckx, T.; Vanherle, S.; Maillieux, J.; Gervois, P.; Wolfs, E.; Dehairs, J.; et al. Stearoyl-CoA desaturase-1 impairs the reparative properties of macrophages and microglia in the brain. *J. Exp. Med.* **2020**, *217*, e20191660. [[CrossRef](#)] [[PubMed](#)]
14. Healy, L.M.; Ho Jang, J.; Won, S.J.; Lin, H.; Touil, H.; Aljarallah, S.; Bar-Or, A.; Antel, J.P. MerTK-mediated regulation of myelin phagocytosis by macrophages generated from patients with MS. *Neurol. Neuroimmunol. Neuroinflamm.* **2017**, *4*, e402. [[CrossRef](#)] [[PubMed](#)]
15. Moore, K.J.; Rosen, E.D.; Fitzgerald, M.L.; Randow, F.; Andersson, L.P.; Altshuler, D.; Milstone, D.S.; Mortensen, R.M.; Spiegelman, B.M.; Freeman, M.W. The role of PPAR-gamma in macrophage differentiation and cholesterol uptake. *Nat. Med.* **2001**, *7*, 41–47. [[CrossRef](#)] [[PubMed](#)]
16. Reichert, F.; Rotshenker, S. Complement-receptor-3 and scavenger-receptor-AI/II mediated myelin phagocytosis in microglia and macrophages. *Neurobiol. Dis.* **2003**, *12*, 65–72. [[CrossRef](#)]
17. Argmann, C.A.; Sawyez, C.G.; McNeil, C.J.; Hegele, R.A.; Huff, M.W. Activation of peroxisome proliferator-activated receptor gamma and retinoid X receptor results in net depletion of cellular cholesteryl esters in macrophages exposed to oxidized lipoproteins. *Arterioscler. Thromb. Vasc. Biol.* **2003**, *23*, 475–482. [[CrossRef](#)]
18. Chinetti, G.; Lestavel, S.; Bocher, V.; Remaley, A.T.; Neve, B.; Torra, I.P.; Teissier, E.; Minnich, A.; Jaye, M.; Duverger, N.; et al. PPAR-alpha and PPAR-gamma activators induce cholesterol removal from human macrophage foam cells through stimulation of the ABCA1 pathway. *Nat. Med.* **2001**, *7*, 53–58. [[CrossRef](#)]
19. Van Boxel-Dezaire, A.H.; Hoff, S.C.; van Oosten, B.W.; Verweij, C.L.; Dräger, A.M.; Adèr, H.J.; van Houwelingen, J.C.; Barkhof, F.; Polman, C.H.; Nagelkerken, L. Decreased interleukin-10 and increased interleukin-12p40 mRNA are associated with disease activity and characterize different disease stages in multiple sclerosis. *Ann. Neurol.* **1999**, *45*, 695–703. [[CrossRef](#)]
20. Rieckmann, P.; Albertch, M.; Kitze, B.; Weber, T.; Tumani, H.; Broocks, A.; Luer, W.; Helvig, A.; Poser, S. Tumor necrosis factor-alpha messenger RNA expression in patients with relapsing-remitting multiple sclerosis is associated with disease activity. *Ann. Neurol.* **1995**, *37*, 82–88. [[CrossRef](#)]
21. Khaibullin, T.; Ivanova, V. Elevated levels of proinflammatory cytokines in cerebrospinal fluid of multiple sclerosis patients. *Front. Immunol.* **2017**, *8*, 531. [[CrossRef](#)] [[PubMed](#)]
22. Lees, J.R.; Cross, A.H. A little stress is good: IFN-gamma, demyelination, and multiple sclerosis. *J. Clin. Investig.* **2007**, *117*, 297–299. [[CrossRef](#)] [[PubMed](#)]
23. Chu, C.Q.; Wittmer, S.; Dalton, D.K. Failure to suppress the expansion of the activated CD4 T cell population in interferon gamma-deficient mice leads to exacerbation of experimental autoimmune encephalomyelitis. *J. Exp. Med.* **2000**, *192*, 123–128. [[CrossRef](#)] [[PubMed](#)]
24. Panitch, H.S.; Haley, A.S. Exacerbations of multiple sclerosis in patients treated with gamma interferon. *Lancet* **1987**, *1*, 893–895. [[CrossRef](#)]
25. Panitch, H.S.; Hirsch, R.L.; Schindler, J.; Johnson, K.P. Treatment of multiple sclerosis with gamma interferon: Exacerbations associated with activation of the immune system. *Neurology* **1987**, *37*, 1097–1102. [[CrossRef](#)]
26. Niino, M.; Iwabuchi, K.; Kikuchi, S.; Ato, M.; Morohashi, T.; Ogata, A.; Tashiro, K.; Onoe, K. Amelioration of experimental autoimmune encephalomyelitis in C57BL/6 mice by an agonist of peroxisome proliferator-activated receptor-gamma. *J. Neuroimmunol.* **2001**, *116*, 40–48. [[CrossRef](#)]
27. Storer, P.D.; Xu, J.; Chavis, J.; Drew, P.D. Peroxisome proliferator-activated receptor-gamma agonists inhibit the activation of microglia and astrocytes: Implications for multiple sclerosis. *J. Neuroimmunol.* **2005**, *161*, 113–122. [[CrossRef](#)]
28. Schett, G. Physiological effects of modulating the interleukin-6 axis. *Rheumatology* **2018**, *57* (Suppl. S2), ii43–ii50. [[CrossRef](#)]

29. Maillieux, J.; Vanmierlo, T.; Bogie, J.F.J.; Wouters, E.; Lutjohann, D.; Hendriks, J.J.A.; van Horssen, J. Active liver X receptor signaling in phagocytes in multiple sclerosis lesions. *Mult. Scler.* **2018**, *24*, 279–289. [[CrossRef](#)]
30. Kotter, M.R.; Li, W.W.; Zhao, C.; Franklin, R.J.M. Myelin impairs CNS remyelination by inhibiting oligodendrocyte precursor cell differentiation. *J. Neurosci.* **2006**, *26*, 328–332. [[CrossRef](#)]
31. Zhu, Y.; Lyapichev, D.H.L.; Motti, D.; Ferraro, N.M.; Zhang, Y.; Yahn, S.; Soderblom, C.; Zha, J.; Bethea, Z.J.R.; Spiller, K.L. Macrophage transcriptional profile identifies lipid catabolic pathways that can be therapeutically targeted after spinal cord injury. *J. Neurosci.* **2017**, *37*, 2362–2376. [[CrossRef](#)] [[PubMed](#)]
32. Natrajan, M.S.; Komori, M.; Kosa, P.; Johnson, K.R.; Wu, T.; Franklin, R.J.M.; Bielekova, B. Pioglitazone regulates myelin phagocytosis and multiple sclerosis monocytes. *Ann. Clin. Transl. Neurol.* **2015**, *2*, 1071–1084. [[CrossRef](#)] [[PubMed](#)]
33. Wang, N.; Yin, R.; Liu, Y.; Guangmei, Y.L.; Mao, G.; Xi, F. Role of peroxisome proliferator-activated receptor-gamma in atherosclerosis: An update. *Circ. J.* **2011**, *75*, 528–535. [[CrossRef](#)] [[PubMed](#)]
34. Chinetti, G.; Lestavel, S.; Fruchart, J.-C.; Clavey, V.; Staels, B. Peroxisome proliferator-activated receptor alpha reduces cholesterol esterification in macrophages. *Circ. Res.* **2003**, *92*, 212–217. [[CrossRef](#)] [[PubMed](#)]
35. Boren, J.; Brindle, K.M. Apoptosis-induced mitochondrial dysfunction causes cytoplasmic lipid droplet formation. *Cell Death Differ.* **2012**, *19*, 1561–1570. [[CrossRef](#)]
36. Chawla, A.; Boisvert, W.A.; Lee, C.-H.; Laffitte, B.A.; Barak, Y.; Joseph, S.B.; Liao, D.; Nagy, L.; Edwards, P.A. A PPAR gamma-LXR-ABCA1 pathway in macrophages is involved in cholesterol efflux and atherogenesis. *Mol. Cell* **2001**, *7*, 161–171. [[CrossRef](#)]
37. Chinetti, G.; Gbaguidi, F.C.; Griglio, S.; Mallat, Z.; Antonucci, M.; Poulain, P.; Chapman, J.; Frucgart, J.C.; Tedgui, A.; Fruchart, J.N. CLA-1/SR-BI is expressed in atherosclerotic lesion macrophages and regulated by activators of peroxisome proliferator-activated receptors. *Circulation* **2000**, *101*, 2411–2417. [[CrossRef](#)]
38. Diab, A.; Deng, C.; Smith, J.D.; Hussain, R.Z.; Phanavanh, B.; Lovett-Racke, A.E.; Drew, P.D.; Racke, K.M. Peroxisome proliferator-activated receptor-gamma agonist 15-deoxy-Delta(12,14)-prostaglandin J(2) ameliorates experimental autoimmune encephalomyelitis. *J. Immunol.* **2002**, *168*, 2508–2515. [[CrossRef](#)]
39. Szalardy, L.; Zadori, D.; Tanzos, E.; Simu, M.; Bencsik, K.; Vecsei, L.; Klivenyi, P. Elevated levels of PPAR-gamma in the cerebrospinal fluid of patients with multiple sclerosis. *Neurosci. Lett.* **2013**, *554*, 131–134. [[CrossRef](#)]
40. Jorissen, W.; Wouters, E.; Bogie, J.F.; Vanmierlo, T.; Noben, J.-P.; Sviridov, D.; Hellings, N.; Somers, V.; Valcke, R.; Vanwijmeersch, B. Relapsing-remitting multiple sclerosis patients display an altered lipoprotein profile with dysfunctional HDL. *Sci Rep.* **2017**, *7*, 43410. [[CrossRef](#)]
41. Bogie, J.F.; Maillieux, J.; Wouters, E.; Jorissen, W.; Grajchen, E.; Vanmol, J.; Wouters, K.; Hellings, N.; van Horssen, J.; Vanmierlo, T. Scavenger receptor collectin placenta 1 is a novel receptor involved in the uptake of myelin by phagocytes. *Sci. Rep.* **2017**, *7*, 44794. [[CrossRef](#)] [[PubMed](#)]
42. Bogie, J.F.; Stinissen, P.; Hellings, N.; Hendriks, J.J.A. Myelin-phagocytosing macrophages modulate autoreactive T cell proliferation. *J. Neuroinflamm.* **2011**, *8*, 85. [[CrossRef](#)] [[PubMed](#)]
43. Van der Laan, L.J.; Ruuls, S.R.; Weber, K.S.; Lodder, I.J.; Dopp, E.A.; Dijkstra, C.D. Macrophage phagocytosis of myelin in vitro determined by flow cytometry: Phagocytosis is mediated by CR3 and induces production of tumor necrosis factor-alpha and nitric oxide. *J. Neuroimmunol.* **1996**, *70*, 145–152. [[CrossRef](#)]
44. Thompson, A.J.; Banwell, B.L.; Barkhof, B.; Carroll, W.M.; Coetzee, T.; Comi, G.; Correale, J.; Fazekas, F.; Filippi, M.; Fujihara, K. Diagnosis of multiple sclerosis: 2017 revisions of the McDonald criteria. *Lancet Neurol.* **2018**, *17*, 162–173. [[CrossRef](#)]

**Publisher's Note:** MDPI stays neutral with regard to jurisdictional claims in published maps and institutional affiliations.



© 2020 by the authors. Licensee MDPI, Basel, Switzerland. This article is an open access article distributed under the terms and conditions of the Creative Commons Attribution (CC BY) license (<http://creativecommons.org/licenses/by/4.0/>).